A REVIEW ON ANTIMONY-BASED PEROVSKITE SOLAR CELLS

ANKIT S.T.
Department of Chemical Engineering, National Institute of Technology Karnataka, India
ankitsthomas@gmail.com

Abstract - Lead halide perovskites have been the conventionally used perovskite light absorbers over the past decade. However, with the toxicity levels and poor stability to UV radiations, there's an urgent calling for alternative perovskite materials. Antimony-based perovskites have proven to be one such material with unique optoelectronic properties, conventional fabrication processes, low-toxicity levels and high stability values. In this review we look into the structure of Antimony perovskites, the progress that various researchers have made over the recent years and the challenges and opportunities that lie ahead for this budding technology. The review also highlights the various computational, theoretical and experimental studies done by researchers to highlight the peculiar Lead-free perovskite materials and its distinctive features. Although the efficiency levels of these devices are not very high, the improvement the devices have made with remarkable stability characteristics, make it a very viable candidate for commercial perovskite photovoltaics.

Keywords: Perovskite Solar Cells, Photovoltaic Technology, Lead-free Perovskites, Solar Cell Materials, Antimony-based Perovskites

1. INTRODUCTION

Perovskite Solar Cells (PSCs) have attracted a great deal of attention for their unique optoelectronic properties, tuneable energy bandgap, easy fabrication process, abundant material sourcing, cheap and efficient results. The common active material used in a PSC is typically $CH_3NH_3PbI_3$ ($MAPbI_3$ – Methylammonium Lead Iodide).

It is important to note that a perovskite molecule follows the general molecular formula of ABX_3, where A is a large cation typically MA^+ and FA^+. B is a smaller cation usually belonging to the transition group elements (Pb) and X is halide anion (Cl^-, Br^-, F^-). Lead-based perovskites have shown tremendous success over the previous years. The reasons for this are as follows: high absorption coefficient, suitable bandgap, reduced defects, low temperature processability, solution processable and long carrier lifetimes. However, lead-based perovskites cannot be commercialized majorly due to the following reasons: low stability properties towards UV radiation, heat and moisture, and high toxicity levels. This calls for more efficient, sustainable and eco-friendly alternatives [1].

Reports have also conducted tests like Life Cycle Assessments (LCA), to measure the ecological balance, environmental impact and cost-benefit analysis of perovskite solar technologies. This investigates the device fabrication right from sourcing the materials to deposition and finally fabricating the entire device. The results from LCA studies indicate that there is significant contamination occurring due to Pb-based perovskites, especially in the processing stage. Moreover, other reports have suggested that fabricating devices using Pb-based perovskites have resulted in air and water contamination, damage of local ecosystems and degradation of worker's health. Therefore, this gives us more reasons to shift towards greener, safer and highly-efficient perovskite devices [2].

There have been various other alternatives to replace Pb like Bi, Sb, Ge and Sn. It is important to note that, before replacing the Pb in a perovskite material, we need to study the impact of the alternatives on the environment. Sn^{2+} and Ge^{2+} get oxidized easily to Sn^{4+} and Ge^{4+} respectively, which makes it extremely difficult to work with in a PSC. Moreover, Sn-based perovskites are toxic as well. Hence the only viable alternatives are Bi and Sb-based perovskites which belong to same group (VA) in the periodic table. Unlike, Sn and Ge, Bi and Sb are trivalent cations (Bi^{3+} and Sb^{3+}) with an ionic radius very similar to Pb^{2+}. From this section, we can coherently conclude that researchers and policy makers need to develop and come up with a structured framework that investigates alternatives for Pb on a thorough basis, right from processing costs to material sourcing availability [3].

Sb-based halide perovskites have been developed in the past and are being used currently on a very temporary scale. They have been identified as suitable alternatives to behave as light absorbers. $MA_3Sb_2I_9$ and $Cs_3Sb_2I_9$ are few of the common Sb-based light absorbers that have been developed. However, these materials have extremely wide bandgaps, high binding energies and high carrier effective masses, which further limits the photovoltaic performance [1]. This is the predominant reason why VA-based halide perovskites are not being implemented on a large basis with performances much lower than Pb-based perovskites.

In this review, we shall look into how Antimony

perovskites are synthesized. The computational and theoretical studies on Sb-based perovskite materials are also covered in this article and how theoretical and experimental results can be correlated, especially on an optoelectronic basis. The general molecular structure ($A_3Sb_2X_9$) is elaborated upon, along with the recent progress, challenges, barriers to commercialization and further opportunities for research.

2. FABRICATION OF ANTIMONY-BASED PEROVSKITES

Perovskite films are generally produced through solution processable methods. However, they can also be prepared through vapour-assisted methods. The photovoltaic performance depends strongly on the film quality produced, which indirectly depends on the synthesis method. Typically, when a solution processable method is used, factors like age of chemicals, solvent boiling point, atmospheric conditions and coordinating strength, directly impact the film quality and its optoelectronic properties [4].

One-step deposition method is the commonly used method. In this case, halide of salts of A and B cation are dissolved in a polar solvent which is then spin-coated onto a substrate. Perovskite films with larger grain sizes are preferred as they reduce grain boundaries and improve charge transport across the material. The perovskite precursor solutions have solvated ions and colloidal networks that play a direct impact on the crystal growth of the perovskite crystal. The interaction between the metal halides and the solvent molecules plays an important role in determining film morphology. If the species are strongly coordinated, perovskite nucleation and crystal growth tend to slow down. Moreover, the solvent that is also used in one-step deposition plays an important role in perovskite film morphology. There is a technique that is known as antisolvent washing that is used after the perovskite crystals are formed. This is done to remove the perovskite precursor solvents. The choice of antisolvent used also plays a major role in determining the morphology and quality of the film [5].

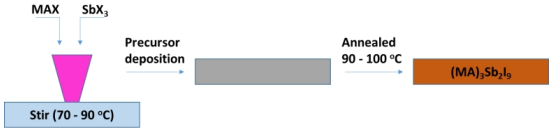

Fig.1. Schematic representation of Sb-film synthesis

Two-step deposition method includes, firstly, deposition of metal halide, followed by interdiffusion of organic salt. Through this method, the film produced is not just homogeneous, it is uniform, has better wettability and has reduced notable defects. It is important for the organic salt to penetrate into the inorganic salt. This ensures that the perovskite film obtained has suitable thickness. The deposition of the first layer can be further improved by using additives and restructuring the metal halides [4]. Figure 1 shows a clear representation of the processes required to synthesize a Pb-free perovskite film.

3. STRUCTURE OF ANTIMONY-BASED PEROVSKITES

As mentioned earlier, Sb being a trivalent cation has three electrons in its valence shell. Thus, when a trivalent cation replaces Pb^{2+}, the resulting ionic compound formed will be of the form SbX_6^{3-}. This is an octahedron shaped molecule where halide ions are coordinated to the A cation to give rise to a perovskite molecule with different dimensionality and structure. The molecular formula of $A_3B_2X_9$ usually produces perovskite molecules that are 0-dimensional (0D) or 2-dimensional (2D) [1]. However, in the case of double perovskites with a molecular formula of $A_2B^IB^{III}X_6$ have a 3-dimensional (3D) structure where the B^I and B^{III} cations are corner sharing molecules.

Sb-based perovskites are known to possess extremely unique and exceptional optoelectronic properties when incorporated into a PSC. Moreover, these materials have been tested from a computational and experimental setup to study the optic properties of 0D and 2D forms.

0D is a dimeric form and 2D is a layered form of the $Cs_3Sb_2I_9$. In a hypothetical scenario, $CsSbI_3$ can be produced by structurally modifying the $Cs_3Sb_2I_9$ layers [6]. 2D $Cs_3Sb_2I_9$ has an optical bandgap of 2.05 eV and is regarded for its enhanced stability in ambient conditions when compared to $MAPbI_3$. The Cs atom can be replaced with other alkali atoms like Rb or K. It is important to note here that the A cation plays a very important role in the optoelectronic properties of the material. It can impact the bandgap by tuning it to a direct or indirect bandgap. Rb and K-based Sb halide perovskites have a direct bandgap and have a 2D structure due to their smaller ionic radius which stabilizes the 2D structure [7]. Colloidal $Cs_3Sb_2I_9$ and $Rb_3Sb_2I_9$ nanocrystals have been synthesized previously, with high absorption coefficients and a 2D structure [8]. Thus, making them suitable candidates as perovskite light absorbers.

A Cu-doped Sb-based halide perovskite was recently synthesized with an indirect bandgap of 1.02 eV. This was compared to that of $Cs_2SbAgCl_6$ with a bandgap of 2.65 eV [9]. Double-layered perovskites with the molecular formula of $Cs_{3+n}M(II)_nSb_2X_{9+3n}$ with octahedral layers of [GeI_6] and [SnI_6]. This modification resulted in enhanced structural stability, increased electronic dimensionality, reduced bandgap and binding energies, and higher absorption properties [10]. Vargas and coworkers developed a Mn and Cu, Sb-based halide perovskite. Through this study it was shown that on varying the Mn and Cu ratios, the bandgap of the perovskite molecule can be adjusted. In addition to this, physical characteristics like magnoelectric properties can be tuned using molecular, sidechain or compositional engineering [11].

Jakubas and Bagautdinov's works suggested that they synthesized $MA_3Sb_2I_9$ and $Cs_3Sb_2I_9$, respectively and studied their corresponding properties [12,13]. Yang and coworkers showed and concluded that by replacing I^- with Br^-, the resulting perovskite possesses a triagonal crystal

structure [14]. Zhang and coworkers synthesized $(NH_4)_3Sb_2I_9$ and showed that it crystallizes in a monoclinic crystal form [15]. Zuo and coworkers synthesized $(NH_4)_3Sb_2I_9$ through an antisolvent vapor-assisted crystallization method. Through this procedure, the resultant perovskite molecule formed an octahedron with Nitrogen atoms at the centre forming a tetrahedron [16].

Buonassisi and coworkers studied the optoelectronic and photovoltaic properties of $Cs_3Sb_2I_9$, $K_3Sb_2I_9$ and $Rb_3Sb_2I_9$ perovskite materials. It was found that the materials possessed a 0D, 2D and 2D crystal structure respectively [7]. Table 1 shows a detailed understanding of the film characteristics of various Sb-based perovskites, its film and crystal properties and variation with charge carrier type.

Table 1. Charge carrier mobility of Antimony perovskites

Material	Film type	Charge carrier type	Charge carrier mobility ($cm^{-1} V^{-1} s^{-1}$)	Ref.
$(MA)_3Sb_2I_xBr_{9-x}$	Single crystal	Electron	12.3	[17]
$(MA)_3Sb_2I_xBr_{9-x}$	Single crystal	Hole	4.8	[17]
$(MA)_3Sb_2I_9$	Single crystal	Hole	4.8	[17]
$(MA)_3Sb_2I_9$	Single crystal	Electron	12.3	[17]
$(MA)_3Sb_2I_9$	Film	Hole	1.2×10^{-4}	[17]
$(MA)_3Sb_2I_9$	Film	Electron	1.5×10^{-4}	[17]

4. COMPUTATIONAL STUDIES ON ANTIMONY-BASED HALIDE PEROVSKITES

Sb-based double perovskites have been studied theoretically and computationally using certain analysis like DFT/LDA. The results showed that majority of the double perovskites possessed an indirect bandgap. However, these could be converted to a direct bandgap through suitable modifications and experimental strategies.

A total of eleven double perovskites were developed and were screened on the basis of thermodynamic stability, optoelectronic stability, bandgap values, etc. $Cs_2InSbCl_6$ was one of the two materials that displayed a direct bandgap of 1.0 eV [18]. Deng and coworkers produced a double perovskite $Cs_2AgSbCl_6$. As per computational results, the material showed an indirect bandgap of 2.41 eV. The experimental results show a similar value of 2.60 eV. Coupling $Cs_2AgSbCl_6$ with TiO_2 heterostructures showed improved light absorption properties [. Sb_2S_3, $Cs_2Sb_8S_{13}$ and $MA_2Sb_8Sb_{13}$ are few of the other compounds that have been investigated for its unique structure and electronic properties [19]. Through computational results, the observed bandgap values were 1.72, 1.85 and 2.08 eV, respectively. Deng and coworkers also synthesized an Antimony-Silver double perovskite of the formula $(CH_3NH_3)_2AgSbI_6$ with a bandgap of 1.93 eV and enhanced stability of 370 days [20].

Computational results have also shown that a mixed-metal-halide perovskite: $(CH_3NH_3)_2AgSbI_6$ possessed a bandgap of 2.0 eV. This value was verified through experimental results by synthesizing MA_2AgSbI_6 with a bandgap of 1.93 eV [20].

VA-based halide perovskites (Bi and Sb) have been suggested as alternatives to Pb-halide perovskites. The reasons for this transition are as follows: a) low toxicity, b) high structural stability, c) greater UV, moisture and temperature stability. These advantages and the rate at which these materials are progressing in recent times, improved PCE and commercialization will be definitely possible in the long run. Figure 2 depicts a typical device employing Sb-based perovskite layer as the light absorber and the corresponding energy level diagram for all the device components.

Zuo and coworkers showed that $(NH_4)_3Sb_2I_9$ has an optical bandgap of 2.27 eV [21], whereas Boopathi and coworkers showed that $Cs_3Sb_2I_9$ has a bandgap of 1.95 eV and $MA_3Sb_2I_9$ has a bandgap of 2.0 eV [22]. Buonassisi and coworkers found that the optical bandgap of Cs, Rb and K-based Sb-Iodide perovskites are 2.43, 2.03 and 2.02 eV, respectively, through UV-Vis absorption spectroscopy.

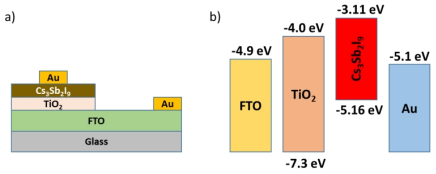

Fig.2. a) Schematic diagram of Cs-Sb PSC, b) Energy level diagram of device materials

5. ANTIMONY HALIDE PSCs

5.1. $Cs_3Sb_2I_9$ Perovskites

As mentioned earlier, Sb can form a number of varied organic and inorganic cations. $Cs_3Sb_2I_9$ forms different solid structures. The solution processed form is a 0D structure whereas the 2D-layered structure is formed through solid or gas reactions. It was back in 2015 when $Cs_3Sb_2I_9$ was first used as a light absorber. Saparov and coworkers determined that the 2D structure has a bandgap of 2.05 eV, absorption coefficient of 10^5 cm^{-1} and ionization potential of 5.6 eV. The stability reported is much higher than $MAPbI_3$ especially in ambient atmospheres. The PCE produced using $Cs_3Sb_2I_9$ as a light absorber was less than 1%. This is because of its high recombination probability and defect states [23].

Similarly, the 0D structure (bandgap of 2.0 eV) was also used in PSCs. Chu and coworkers developed a planar PSC device to obtain a PCE of 0.67% [24]. On using HI as an additive, the device produced a PCE of 0.84% and a V_{oc} of 0.60 V. However, Correa-Baena and coworkers showed that the low photocurrent values are attributed to its indirect bandgap and high binding energy [25]. Furthermore, a layered and dimeric variant of $Cs_3Sb_2I_9$

was prepared through a vapor-assisted solution processable method. The lifetime and binding energy value were found to be 6 ns and 100 meV respectively, for the layered variant. Including the layered and dimeric form into a PSC yielded a PCE of 1.5% and 0.89%, respectively [26]. Zhou and coworkers synthesized a $MA_3Sb_2Cl_xI_{9-x}$ by adding Methylammonium Chloride into the precursor solution [27].

The $Cs_3Sb_2I_9$ films formed are of very high film quality and tend to exist in the dimeric form. Zhubing He and coworkers attempted to solve this issue by using Hydrochloric Acid (HCl) as an additive [28]. Using this method, Chlorine behaved as an inhibitor to resist the Sb-I-Sb bond formation. This eventually produced a layered $Cs_3Sb_2I_9$ film with a bandgap of 2.05 eV. It is important to note that the observed bandgap value is lower than its dimeric form (2.47 eV). Incorporating the layered structure into a PSC produced a PCE of 1.21% whereas the dimeric form produced only 0.43%. This variation in PCE level can be attributed to the reduced trap states, improved carrier mobility and junction quality. The addition of HCl essentially resolved the dimeric form nature of $Cs_3Sb_2I_9$.

Umar and coworkers fabricated mesoporous PSCs using $Cs_3Sb_2I_9$ [28]. In this study, a dimer phase was produced and a layered phase was produced using HCl. The films were also synthesized with and without antisolvents. The results showed that, presence of antisolvents, especially isopropanol, yielded films with reduced pinholes and trap states. The highest PCE obtained was of 1.21%, from a device using HCl. Singh and coworkers produced a modified $Cs_3Sb_2I_9$ phase (layered polymorph phase) [26]. On incorporating this material into a PSC, the photovoltaic performance was 1.5%, which was higher than its dimer counterpart. The improved photovoltaic performance can be related to the lower bandgap values and unique optoelectronic properties that the layered structure possesses.

Moreover, Chonamada and coworkers also studied the stability characteristics of layered and dimer form of $Cs_3Sb_2I_9$ profoundly [29]. Figure 5 shows an accurate flowchart-based representation on how the layered and dimeric forms of $Cs_3Sb_2I_9$ perovskite materials can be synthesized. The stability was studied under humidity, light and heat. Through the humidity studies, it was observed that both the films hydrated and decomposed into CsI, Sb_2O_3 and HI. When HI was added, the reaction was seen to be reversed. Through the thermal studies, it was noted that both the films decomposed to SbI_2 and CsI which can be recovered easily. However, the vital point to note here is that, the layered variant showed greater stability against heat. Under the light studies, both the films began to decompose through photoinduced degradation. Once these samples were stored in a dark environment, no notable degradation was noted. It was observed that the dimer form of the material degraded after 49 days whereas the layered form degraded only after 88 days. These results further validate why $Cs_3Sb_2I_9$ is a viable candidate as a light absorber for photovoltaic applications.

5.2. $Rb_3Sb_2I_9$ Perovskites

Harikesh and coworkers developed a solution processable method of the same Sb-based perovskite, however, the Cs atom was replaced by Rb [30]. Moreover, due to the smaller ionic radius of Rb, the resulting perovskite will be of a layered structure. Similar to its Cs-counterpart, the Rb-Sb-based perovskite displayed enhanced thermal stability which is a useful property in a PSC. However, its large indirect bandgap (2.1 eV) makes it unfavourable for optimal photovoltaic performance. Coupling this material along with poly-TPD as the HTM resulted in a PCE of 0.66%.

From the above work, one can conclude that the A cation plays more than just a significant role in determining photovoltaic performance. A cation can directly or indirectly impact the structural and optoelectronic properties of produced films. Moreover, it also influences the exciton binding energy, carrier charge effective masses and produced photocurrents. The largest efficiency obtained by using a Rb-based Sb perovskite is 0.76% [7]. Weber and coworkers showed that the crystal structure is not affected by replacing the Iodide ion with Bromide [31]. However, there is a notable increase in the bandgap and the PCE obtained is nearly 1.3%. Additionally, there is a notable improvement in device stability for up to 150 days and 85% of its initial PCE is retained.

$Rb_3Sb_2I_9$ is a potential candidate for PSCs due to its favourable absorption coefficient and improved stability properties. The incorporation of Rb as an A-site cation improves the structural, dimensional and optical properties of the material, influences the binding energy and eventually the photovoltaic performance of the material. Buonassisi and coworkers fabricated PSCs using K, Rb and Cs-based Sb-halide perovskites. The results showed that the Rb-based device exhibited improved device efficiency and the K and Cs-based device showed lower efficiency values.

A perovskite film with a large grain size directly impacts the device performance to improve carrier mobility and lifetime. Therefore, the photovoltaic performance using various materials can be directly improved by tuning charge mobility values, diffusion lengths and carrier drift. Li and coworkers synthesized $Rb_3Sb_2I_9$ using various methods and studied the dependency of photovoltaic performance on synthesis methods [32]. It was observed that the highest device performance was obtained from the high-temperature vapour annealing method (HTVA) with a grain size of 600 nm. The increase in device efficiency can be associated to the larger grains, greater carrier mobility and lifetime values.

5.3. $MA_3Sb_2I_9$ Perovskites

Hebig and coworkers synthesized solution processable $MA_3Sb_2I_9$, which possess a hexagonal shape [33]. Moreover, amorphous $MA_3Sb_2I_9$ shows an

absorption coefficient in the range of 10^5 cm^{-1}, optical bandgap of 2.14 eV and large energy disorder. Currently, all the synthesized Sb-based pure halide perovskites have shown bandgaps greater than 2 eV. The $MA_3Sb_2I_9$ film produced through one-step method produced a crystalline film. Whereas, the film produced through a two-step method was amorphous in nature. This amorphous nature can be attributed to the presence of Toluene. Moreover, the hexagonal structure of $MA_3Sb_2I_9$ was visible in the one-step method but a pinhole free and non-hexagonal structure was obtained in the two-step method [34].

There have been studies where the incorporation of $MA_3Sb_2I_9$ into a planar PSC produced a PCE of 0.49% and a V_{oc} of 896 mV. The device components used in this case was: ITO/PEDOT:PSS/$MA_3Sb_2I_9$/PC61BM/ZnO-NP/Al [34]. Giesbrecht and coworkers synthesized the 2D form of $MA_3Sb_2I_9$ in a glovebox using Antimony Acetate [35]. The results showed that the 2D version produced improved results than its 0D counterpart. The PSCs were fabricated through two variants, mesoporous TiO_2 and compact SnO_2 (c-SnO_2). It was observed that the mesoporous-based device yielded higher efficiency values (0.54%) than the c-SnO_2 device (0.36%). However, the higher V_{oc} value was reported for the c-SnO_2-based device due to its lower recombination rates and high film quality.

Shaikh and coworkers synthesized $MA_3Sb_2I_9$ using a two-step sequential deposition method with an indirect bandgap of 2.1 eV [36]. On fabricating a PSC device with this material, a moderate PCE of 0.54% was obtained with a V_{oc} of 740 mV. These values were higher than the devices produced through a one-step deposition method. The higher photovoltaic performance is attributed to the improved film quality, surface morphology, homogeneity, charge extraction and transportation.

Studies have been conducted where PSCs were fabricated using a Cu@NiO as a hole transporting material and ZnO as the electron transporting material [34]. The active layer used in this case was $MA_3(Sb_{1-x}Sn_x)_2I$ and the highest efficiency obtained in this case was 2.69%. This research work showed that $MA_3Sb_2I_9$ has favourable bandgap and morphological features which make it suitable for PSCs. Figure 3 displays the device architecture of one of the highest performing Sb-based devices, where the addition of Pyrene, HI and Chlorobenzene are pointed out clearly.

As discussed previously, using MA^+ as the A site cation produces only the dimeric 0D form. However, the materials large energy disorder and high binding energy results in reduced photocurrent values and PCE values lower than 0.5%. Boopathi and coworkers showed that by using Hydroiodic Acid (HI) as an additive with varying precursor concentrations, the optimal device efficiency is found to be 2.04% and 1.11% for a device without HI additive [34].

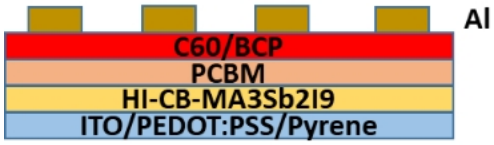

Fig.3. Sb PSC with a hydrophobic layer, HI and Chlorobenzene as additives

It is very evident that the morphology of the film plays a very important role in device performance. Karuppuswamy and coworkers synthesized large grain crystals of $MA_3Sb_2I_9$ [37]. The technique employed by them involved a growth regulation technique wherein HI was used as the additive, chlorobenzene antisolvent treatment and using a hydrophobic HTM. The fabricated device showed reduced voids and improved film quality. The resultant efficiency was 2.77% with reduced interfacial resistance than the standard PEDOT:PSS device. Dai and coworkers showed how $MA_3Sb_2I_{9-x}Cl_x$ 2D films can be produced by using a Lithium bi(trifluoromethane)sulfonamide (Li-TFSI). The resultant efficiency was greater than 3% which is the highest PCE recorded for a pure Sb-based PSC [38]. The resulting material has a bandgap of 2.05 eV, yields a PCE of 3.34 % and enhanced stability of more than 1400 hours in ambient conditions. The reasons for improved stability and device performance can be related to 2D perovskite strain relaxation, thermodynamic stability, better crystallinity and barrier separation to oxygen and moisture.

Due to Sb's smaller effective ionic radius when compared to Pb and Sn, there are suitable optoelectronic properties that develop it to become a suitable active layer. Bromoantimonates containing Sb in both valence states (III and V) produced a PCE of nearly 4%. The regular configuration of PSCs shows better performance than the inverted structure. This was confirmed by the findings from Baranwal and coworkers [39]. They used a PSC device architecture of TiO_2/$(CH_3NH_3)_3Sb_2I_9$/spiro-OMeTAD and NiO/$(CH_3NH_3)_3Sb_2I_9$/PCBM. It was found that the device efficiency was greater in the case of the former. Typically, Sb-based halide perovskites have enhanced stability especially towards ambient and thermal conditions. However, the fabricated devices lack in the efficiency which can be related to the poor film quality, poor surface morphology and aggravated pinhole formation.

In order to reduce the bandgap of Sb-based perovskites, research is being carried out on useful doping strategies or material engineering (A-site cation replacement). Pal and coworkers showed that by introducing Sn^{2+} into $MA_3Sb_2I_9$ can reduce the bandgap by 0.45 eV [40]. However, this was not received well because the decrease in bandgap introduced greater surface roughness. Thus, using an optimal Sn^{2+} content, the resultant device had a balance between surface roughness and bandgap value. Eventually, the resulting device produced a PCE greater than 2.65%. Additionally, doping $MA_3Sb_2I_9$ with Sulfur was also used as a potential light absorber [41]. The resulting device using Sulfur as a

dopant produced an efficiency greater than 3.0%.

5.4. $(NH_4)_3Sb_2I_9$ Perovskites

A perovskite-based material of the molecular formula $(NH_4)_3Sb_2I_xBr_{9-x}$ was synthesized [42]. It was found that, on varying the value of x between 0 and 9, the material was tuned in terms of absorption edges, mobility values and consequently V_{oc} values.

Zuo and coworkers optimized NH_4-based Sb-halide perovskites by synthesizing a series of perovskite materials with varying composition [43]. Through this work it was found that the optical bandgap values varied from 2.27 eV to 2.78 eV. Moreover, on using these varied materials for fabricating a device, the highest record efficiency was 0.51%. Although the efficiency values might be poor in nature, the obtained V_{oc} values were significant with the highest value being 1003 mV. Figure 4 is a schematic representation of a device using $(NH_4)_3(Sb_{(1-x)}Bi_x)_2I_9$ as the perovskite material, for a switchable photovoltaic study.

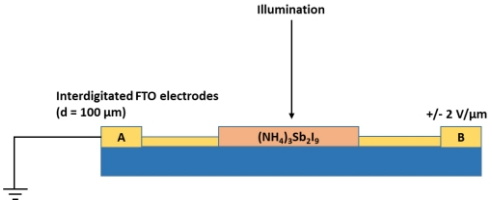

Fig.4. Device configuration with light absorber as $(NH_4)_3(Sb_{(1-x)}Bi_x)_2I_9$

5.5. Other Sb-based Perovskites

Sb halide-based double perovskites is a domain that is under constant development as they have been considered as the next best material to replace Pb-based PSCs. Karmakar and coworkers showed that Cu^{2+} doping can reportedly improve $Cs_2SbAgCl_6$ perovskite performance [44]. The resulting feature showed a reduced indirect bandgap from 2.6 eV to 1.0 eV. Moreover, the device displayed intense structural, photophysical, thermal and moisture stability for more than a year. Using electronic dimensionality principles, by inserting $[M^{II}X_6]$ layers to $Cs_3Sb_2X_9$, double perovskites can be synthesized with lower bandgaps and carrier effective masses. Recently, $FA_4GeSbCl_{12}$ double perovskite was produced with a direct bandgap of 1.3 eV [45]. The resulting layer produced a stable and efficient device with a PCE greater than 4.5%.

Adonin and coworkers studied the implementation of N-ethylpyridinium bromoantimonate (N-EtPy) $[SbBr_6]$ in PSCs [46]. The material was implemented in an inverted PSC, with a bandgap of 2.25 eV, (N-EtPy) $[SbBr_6]$ is a potential candidate for tandem solar cells. (N-EtPy) $[SbBr_6]$ was used in PSCs with different ETMs (TiO_2 and PCBM). The TiO_2 corresponds to the standard regular device architecture whereas PCBM corresponds to the inverted architecture. The results showed that the standard device yielded a higher device efficiency of 3.8% due to better charge extraction and transportation properties.

Li and coworkers synthesized various 0D Sb-containing perovskite like materials. The objective of the research was to identify potential compounds with lower bandgap values to fabricate a high-efficiency PSC [47]. Through this work, two heteromorphic hybrid compounds of Sb were identified with bandgap values suitable for photovoltaic applications. Jia and coworkers synthesized Cu_3SbI_6 with an indirect bandgap of 2.43 eV [48]. The fabricated device produced a PCE of 0.50% and a V_{oc} value of 704 mV. Vargas and coworkers synthesized a Cu-Sb-based halide perovskite with a direct bandgap of 1.02 eV [49]. $Cs_4CuSb_2Cl_{12}$ displayed excellent stability characteristics, favourable optoelectronic properties and a narrow bandgap.

Nie and coworkers reported a similar structure but with a S-Sb mix to produce $MASbSI_2$ [50]. The device fabricated using this perovskite-like compound produced a device efficiency of 3.08%. Moreover, the unencapsulated devices showed excellent stability properties where 90% of its initial PCE was retained after dark condition storage. Table 2 shows a short summary of the notable Sb-based PSCs which have produced reasonable efficiency values over the recent years. In the table 2, PEPDTBT is (poly(2,6-(4,4-bis-(2-ethylhexyl)-4H-cyclopenta[2,1-b;3,4-b']dithiophene)-alt-4,7(2,1,3-benzothiadiazole)).

Table 2. Photovoltaic performance of notable Antimony Halide PSCs

Device structure	PCE (%)	J_{sc} (mA/cm^2)	V_{oc} (V)	Ref.
ITO/PEDOT:PSS/$Cs_3Sb_2I_9$/PCBM/C60/BCP/Al	0.84	2.91	0.60	[22]
FTO/TiO_2/$Cs_3Sb_2I_9$/Au	1.21	3.55	0.61	[27]
FTO/TiO_2/m-TiO_2/$Rb_3Sb_2I_9$/spiro-OMeTAD/Au	1.37	4.25	0.55	[30]
ITO/PEDOT:PSS/$Cs_3Sb_2I_9$/PCBM/Al	1.50	5.31	0.72	[25]
ITO/PEDOT:PSS/$MA_3Sb_2I_9$/PCBM/C60/BCP/Al	2.04	5.41	0.62	[22]
FTO/TiO_2/m-TiO_2/$MA_3Sb_2I_{9-x}Cl_x$/spiro-OMeTAD/Au	2.19	5.04	0.69	[26]
ITO/Cu:NiO/$MA_3(Sb_{1-x}Sn_x)_2I_9$/ZnO/Al	2.70	8.32	0.56	[37]
FTO/PEDOT:PSS/Pyrene/$MA_3Sb_2I_9$/PCBM/C60/Al	2.77	6.64	0.7	[36]
FTO/TiO_2/m-TiO_2/$MASbSI_2$/PEPDTBT/Au	3.08	8.12	0.65	[50]
FTO/TiO_2/$MA_3Sb_2I_{9-x}Cl_x$/spiro-OMeTAD/Au	3.34	7.38	0.70	[39]
FTO/TiO_2/$FA_4GeSbCl_{12}$/spiro-OMeTAD/Au	4.70	23.1	0.65	[45]

6. CHALLENGES AND IMPROVEMENT OF ANTIMONY-BASED PEROVSKITES

The major obstacle that refrains Sb from being commercialized is the transition from lab-scale work to a commercial/large-scale work. Factors like instability concerns, device structure and structural stability, lead to hampering in device performance. Along with this, the usual difficulty of hysteresis still exists. Therefore, it is necessary for researchers to focus and develop strategies that not just address these issues but pay maximum detail to Pb-free perovskites.

Over the past few years, research has been actively carried out in the domain of phase transition and structural properties of perovskites. The reaction and

response of Pb-free perovskites to various environmental conditions have been actively studied. Mechanisms to reduce and suppress degradation mechanisms and develop greater solutions are constantly on the loop. In this section, we shall analyse the various methods through which Pb-free perovskites, particularly, Sb-based perovskites decompose or begin to degrade.

Light is one such source that can initiate the decomposition of the perovskite layer. This was proved by various studies. It was later on proved that oxygen and heat also impact hybrid perovskite structures as well. Studies have also concluded that devices in the absence of oxygen, when exposed to elevated temperatures, experience rapid degradation. The result indicates that the perovskite film decays and leaves behind a residue as the final product.

Humidity and moisture critically impact device stability and it has been shown that a perovskite film can be destroyed in a matter of minutes when exposed to highly ambient conditions. Usually, when a varied metal atom is used apart from Pb, studies are focussed on: additional degradation pathways, monitoring device stability, long-term operation of the device, and road to commercialization.

In the case of Sb-based perovskites, the film formation may not be of exceptional quality. This consequently affects the crystallization process, film quality and charge transport/extraction properties. The produced film in this case often contains a lot of pinholes, irregular grain boundaries, unfavourable morphology and uneven thickness/film. Techniques like incorporating additives, partial substitution, low-dimensioned production and deoxidizers have been used. Table 3 displays a summary of Sb-based PSCs.

Table 3: Stability of Antimony-based PSCs

Material	PCE (%)	Stability properties	Ref.
$Cs_3Sb_2I_9$	< 1.0	More stable in ambient conditions than $MAPbI_3$	[6]
MA_2AgSbI_6	-	Stable at room temperature for 370 days (20-60% humidity)	[20]
$MASbSI_2$	3.08	90% of initial PCE is retained after 15 days of dark storage (60% humidity and 25 °C)	[50]
$(NH_4)_3Sb_2I_9$	0.51	80% of initial PCE is retained in a glovebox for 40 days (O_2 < 10 ppm, H_2O < 0.1 ppm). Lost performance entirely at 50% humidity	[17]

Techniques like surface passivation, partial substitution, additives and deoxidizers have been used to address the stability concerns of Sb-based perovskites. Surface passivation is a technique where defects or recombination sites present on the surface of the perovskite film are eradicated through a molecular-binding technique [51]. This method is highly beneficial to reduce charge recombination and promote charge transfer to a greater extent. Using this method, the improvement in device efficiency will be gradual, steady but notable as there is a considerable change in crystal structure. Surface passivation is known to effectively stabilize perovskite nanocrystals.

Partial substitution involves the tuning of the perovskite molecule with atoms/compounds that can modulate the perovskite material properties [52]. This modulation can happen in terms of stability, film formation and efficiency. These improved properties can be observed notably through partially substituting either the A, B or X ions, as they have a significant contribution to device performance.

Additives and deoxidizers are used majority of the times to facilitate better stability properties. Additives can either be organic or inorganic chemicals which are added in a regulated amount to the perovskite solution. Some of the notable examples include: Ammonium Chloride (NH_4Cl) and 2,2,2-trifluoroethylamine hydrochloride (TFEACI) [53,54]. Reducing agents or deoxidizers are commonly used to restrict the oxidation process of metal ions [55]. Examples include: Ascorbic acid, Hydrazine and Hydrophosphorous acid. Moreover, in ideal cases, deoxidizers play a dual role wherein they behave as oxygen scavengers and also as phase separation inhibiter [56].

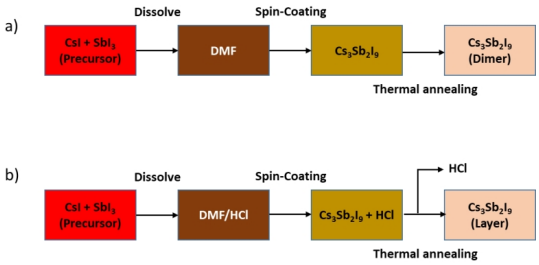

Fig.5. Flowchart representing antisolvent preparatory method for layered and dimeric form of $Cs_3Sb_2I_9$

6. CONCLUSIONS

Through this review, we are able to identify the need for computational and experimental calculations, especially in the field of Sb-based perovskite solar cells. Moreover, we also examined the various works and strategies that researchers have used to improve device performance. The concept was further expanded to double perovskites as well.

It is necessary to highlight that, be it for any perovskite film, the device performance is dependent on the perovskite structure, vacancy states, optoelectronic material properties, binding energy, diffusion lengths and structural properties. In majority of the cases, it is difficult to find a material that is favourable in all these categories.

Thus, techniques like doping, material engineering, compositional engineering and lattice dimension modifications need to be implemented to develop a robust Sb-based perovskite for improved photovoltaic performances. However, the work is not just limited to material characteristics but can be expanded to the deposition and preparation methods. Novel methods are always on the rise to modulate and regulate the perovskite crystal size.

In this review, we are able to conclude the pressing need to use computational and theoretical studies coupled with experimental studies to verify certain findings. These findings are the instability associated with the material or device, need for doping and engineering modifications, long-term stability and barriers to commercialization. Dubey and coworkers have suggested that the path for perovskite solar cells is immense particularly due to the amount of research pending in solvent and precursor selection, film thickness, temperature, growth condition and additive studies [57]. Moreover, Zhang and Gao's works suggested that the incorporation of low bandgap polymers above the perovskite layer is a viable strategy to improve photovoltaic performance [58,59].

The major challenges of Sb-based perovskite materials are: a) wide bandgaps, b) poor morphology, c) incompatible charge transport materials, d) water sensitive. Thus, research needs to continue in a direction to insert less-toxic metals, suitable antisolvents and developing new additives, improve interfacial contact between the perovskite and charge transport materials and lastly, synthesizing hydrophobic interlayers or incorporating cations to the perovskite structure.

VA-based perovskites are also subject to large bandgaps, phase separation, grain boundaries, interfacial recombination, high defect states and poor performance. Antimony is a one-of-a-kind material which varies between 0D to 3D structures, giving it an enhanced structural dimension and unique optoelectronic properties. Thus, up and coming research should predominantly focus on how these materials can break the above-mentioned barriers to produce eco-friendly devices. Research can also be conducted on how various Sb-synthesized perovskite films perform with a variation in halide and A-site ions as this form an integral part of the device. Lastly, looking into the interface and quality of films produced is of utmost importance. One needs to keep a tab on the film quality produced and how various fabrication strategies can play a vital role in determining the favourable device performance.

REFERENCES

[1]. 1.Jin, Z., Zhang, Z., Xiu, J., Song, H., Gatti, T., & He, Z. (2020). A critical review on bismuth and antimony halide based perovskites and their derivatives for photovoltaic applications: recent advances and challenges. Journal Of Materials Chemistry A, 8(32), 16166-16188. doi: 10.1039/d0ta05433j.

[2]. 2.Leccisi E and Fthenakis V, Life-cycle environmental impacts of singlejunction and tandem perovskite PVs: a critical review and future perspectives. Prog Energy 2:032002 (2020).

[3]. 3.Schileo G and Grancini G, Lead or no lead? Availability, toxicity, sustainability and environmental impact of lead-free perovskite solar cells. J Mater Chem C 9:67–76 (2021).

[4]. 4.Thornton, S.T., Abdelmageed, G., Kahwagi, R.F. and Koleilat, G.I. (2022), Progress towards lead-free, efficient, and stable perovskite solar cells. J Chem Technol Biotechnol, 97: 810-829. https://doi.org/10.1002/jctb.6830

[5]. 5.Liao W, Zhao D, Yu Y, Grice CR, Wang C, Cimaroli AJ et al., Lead-free inverted planar formamidinium tin triiodide perovskite solar cells achieving power conversion efficiencies up to 6.22%. Adv Mater 28:9333–9340 (2016).

[6]. 6.B. Saparov, F. Hong, J.-P. Sun, H.-S. Duan, W. Meng, S. Cameron, I. G. Hill, Y. Yan and D. B. Mitzi, Chem. Mater., 2015, 27, 5622-5632.

[7]. 7.J.-P. Correa-Baena, L. Nienhaus, R. C. Kurchin, S. S. Shin, S. Wieghold, N. T. Putri Hartono, M. Layurova, N. D. Klein, J. R. Poindexter, A. Polizzotti, S. Sun, M. G.Bawendi and T. Buonassisi, Chem. Mater., 2018, 30, 3734-3742.

[8]. 8.J. Pal, S. Manna, A. Mondal, S. Das, K. V. Adarsh and A. Nag, Angew. Chem. Int. Edit., 2017, 56, 14187-14191.

[9]. 9.A. Karmakar, M. S. Dodd, S. Agnihotri, E. Ravera and V. K. Michaelis, Chem. Mater., 2018, 30, 8280-8290.

[10]. 10.G. Tang, Z. Xiao, H. Hosono, T. Kamiya, D. Fang and J. Hong, J. Phys. Chem. Lett., 2018, 9, 43-48.

[11]. 11.B. Vargas, R. Torres-Cadena, J. Rodríguez-Hernández, M. Gembicky, H. Xie, J. Jiménez-Mier, Y.-S. Liu, E. Menéndez-Proupin, K. R. Dunbar, N. Lopez, P. Olalde-Velasco and D. Solis-Ibarra, Chem. Mater., 2018, 30, 5315-5321.

[12]. 12.Jakubas, R.; Decressain, R.; Lefebvre, J. NMR and Dilatometric Studies of the Structure Phase transitions of (CH3NH3)3Sb2I9, and (CH3NH3)3Bi2I9 Crystal. J. Phys. Chem. Solids 1992, 53, 755−759.

[13]. 13.Bagautdinov, B.; Novikova, M. S.; Aleksandrova, I. P.; Blomberg, M. K.; Chapuis, G. X-ray study of phase transitions in Cs3Sb2I9 crystal. Solid State Commun. 1999, 111, 361−366.

[14]. 14.Yang, Y.; Liu, C.; Cai, M.; Liao, Y.; Ding, Y.; Ma, S.; Liu, X.; Guli, M.; Dai, S.; Nazeeruddin, M. K. Dimension-controlled Growth of Antimony-based Perovskite-like Halide for Lead-free and Semitransparent Photovoltaics. ACS Appl. Mater. Interfaces 2020, 12, 17062−17069.

[15]. 15.Zhang, H.; Fang, L.; Yuan, R.-Z. Triammonium nonaiododiantimonate(III), (NH4)3[Sb2I9]. Acta Crystallogr., Sect. E: Struct. Rep. Online 2005, 61, i70−i72.

[16]. 16.Zuo, C.; Ding, L. Lead-free Perovskite Materials (NH4)3Sb2IxBr9 x. Angew. Chem., Int. Ed. 2017, 56, 6528−6532.

[17]. 17.C. Zuo, L. Ding, Angew. Chem. 2017, 129, 6628.

[18]. 18.X.-G. Zhao, J.-H. Yang, Y. Fu, D. Yang, Q. Xu, L. Yu, S.-H. Wei and L. Zhang, J. Am. Chem. Soc., 2017, 139, 2630-2638.

[19]. 19.R. X. Yang, K. T. Butler and A. Walsh, J. Phys. Chem. Lett., 2015, 6, 5009-5014.

[20]. 20.Li, Y.-J.; Wu, T.; Sun, L.; Yang.; et al. Lead-free and Stable Antimony−Silver-Halide Double Perovskite (CH3NH3)2AgSbI6. RSC Adv. 2017, 7, 35175−35180

[21]. 21.Zuo, C.; Ding, L. Lead-free Perovskite Materials (NH4)3Sb2IxBr9_x. Angew. Chem., Int. Ed. 2017,

56, 6528−6532.
[22]. 22.Boopathi, K. M.; Karuppuswamy, P.; Singh, A.; Hanmandlu, C.; Lin, L.; Abbas, S. A.; Chang, C. C.; Wang, P. C.; Li, G.; Chu, C. W. Solution-Processable Antimony-based Light-absorbing Materials Beyond Lead Halide Perovskites. J. Mater. Chem. A 2017, 5, 20843−20850.
[23]. 23.B. Saparov, F. Hong, J.-P. Sun, H.-S. Duan, W. Meng, S. Cameron, I. G. Hill, Y. Yan and D. B. Mitzi, Chem. Mater., 2015, 27, 5622-5632.
[24]. 24.H. C. Sansom, G. F. S. Whitehead, M. S. Dyer, M. Zanella, T. D. Manning, M. J. Pitcher, T. J. Whittles, V. R. Dhanak, J. Alaria, J. B. Claridge and M. J. Rosseinsky, Chem. Mater., 2017, 29, 1538–1549.J.-P. Correa-Baena, L. Nienhaus, R. C. Kurchin, S. S. Shin, S. Wieghold, N. T. Putri Hartono, M. Layurova, N. D. Klein, J. R. Poindexter, A. Polizzotti, S. Sun, M. G.Bawendi and T. Buonassisi, Chem. Mater., 2018, 30, 3734-3742.
[25]. 25.A. Singh, K. M. Boopathi, A. Mohapatra, Y. F. Chen, G. Li and C. W. Chu, ACS Appl. Mater. Interfaces, 2018, 10, 2566-2573.
[26]. 26.F. Jiang, D. Yang, Y. Jiang, T. Liu, X. Zhao, Y. Ming, B. Luo, F. Qin, J. Fan, H. Han, L. Zhang and Y. Zhou, J. Am. Chem. Soc., 2018, 140, 1019-1027.
[27]. 27.F. Umar, J. Zhang, Z. Jin, I. Muhammad, X. Yang, H. Deng, K. Jahangeer, Q. Hu, H. Song and J. Tang, Adv. Opt. Mater., 2019, 7, 1801368.
[28]. 28.Chonamada, T. D.; Dey, A. B.; Santra, P. K. Degradation Studies of Cs3Sb2I9: A Lead-Free Perovskite. ACS Appl. Energy Mater. 2020, 3, 47−55.
[29]. 29.Harikesh, P. C.; Mulmudi, H. K.; Ghosh, B.; Goh, T. W.; Teng, Y. T.; Thirumal, K.; Lockrey, M.; Weber, K.; Koh, T. M.; Li, S.; Mhaisalkar, S.; Mathews, N. Rb as an Alternative Cation for Templating Inorganic Lead-Free Perovskites for Solution Processed Photovoltaics. Chem. Mater. 2016, 28, 7496−7504.
[30]. 30.S. Weber, T. Rath, K. Fellner, R. Fischer, R. Resel, B. Kunert, T. Dimopoulos, A. Steinegger and G. Trimmel, ACS Appl. Energy Mater., 2019, 2, 539-547.
[31]. 31.Li, F.; Wang, Y.; Xia, K.; Hoye, R. L. Z.; Pecunia, V. Microstructural and Photoconversion Efficiency Enhancement of Compact Films of Lead-Free Perovskite Derivative Rb3Sb2I9. J. Mater. Chem. A 2020, 8, 4396−4406.
[32]. 32.Hebig, J. C.; Kühn, I.; Flohre, J.; Kirchartz, T. Optoelectronic Properties of (CH3NH3)3Sb2I9Thin Films for Photovoltaic Applications. ACS Energy Lett. 2016, 1, 309−314.
[33]. 33.Recent Progress and Challenges in A3Sb2X9-Based Perovskite Solar Cells Khursheed Ahmad and Shaikh M. Mobin ACS Omega 2020 5 (44), 28404-28412 DOI: 10.1021/acsomega.0c04174
[34]. 34.Giesbrecht, N.; Weis, A.; Bein, T. Formation of stable 2D Methylammonium Antimony Iodide Phase for Lead-free Perovskitelike Solar Cells. J. Phys.: Energy 2020, 2, 024007.
[35]. 35.Ahmad, K.; Kumar, P.; Mobin, S. M. A Two-Step Modified Sequential Deposition Method-based Pb-Free (CH3NH3)3Sb2I9 Perovskite with Improved Open Circuit Voltage and Performance. ChemElectroChem 2020, 7, 946−950.
[36]. 36.Karuppuswamy P, Boopathi KM, Mohapatra A, Chen H-C, Wong K-T, Wang P-C et al., Role of a hydrophobic scaffold in controlling the crystallization of methylammonium antimony iodide for efficient lead-free perovskite solar cells. Nano Energy 45:330–336 (2018).
[37]. 37.Y. Yang, C. Liu, M. Cai, Y. Liao, Y. Ding, S. Ma, X. Liu, M. Guli, S. Dai and M. K. Nazeeruddin, ACS Appl. Mater. Interfaces, 2020, 12, 17062-17069.
[38]. 38.A. K. Baranwal, H. Masutani, H. Sugita, H. Kanda, S. Kanaya, N. Shibayama, Y. Sanehira, M. Ikegami, Y. Numata, K. Yamada, T. Miyasaka, T. Umeyama, H. Imahori, S. Ito, Nano Convergence 2017, 4, 26.
[39]. 39.Chatterjee, S.; Pal, A. J. Tin(IV) Substitution in (CH3NH3)3Sb2I9: Towards Low Band Gap Defect-Ordered Hybrid Perovskite Solar Cells. ACS Appl. Mater. Interfaces 2018, 10, 35194−35205.
[40]. 40.Chatterjee, S.; Pal, A. J. Tin(IV) Substitution in (CH3NH3)3Sb2I9: Towards Low Band Gap Defect-Ordered Hybrid Perovskite Solar Cells. ACS Appl. Mater. Interfaces 2018, 10, 35194−35205.
[41]. 41.T. Li, X. Wang, Y. Yan and D. B. Mitzi, J. Physi. Chem. Lett., 2018, 9, 3829-3833
[42]. 42.C. Zuo and L. Ding, Angew. Chem. Int. Edit., 2017, 56, 6528-6532
[43]. 43.Sani F, Shafie S, Lim HN, Musa AO. Advancement on Lead-Free Organic-Inorganic Halide Perovskite Solar Cells: A Review. Materials (Basel). 2018 Jun 14;11(6):1008. doi: 10.3390/ma11061008. PMID: 29899206; PMCID: PMC6024904.
[44]. 44. Jin, Z., Zhang, Z., Xiu, J., Song, H., Gatti, T., & He, Z. (2020). A critical review on bismuth and antimony halide based perovskites and their derivatives for photovoltaic applications: recent advances and challenges. Journal Of Materials Chemistry A, 8(32), 16166-16188. doi: 10.1039/d0ta05433j
[45]. 45.W. B. Dai, S. Xu, J. Zhou, J. Hu, K. Huang and M. Xu,Sol. Energy Mater. Sol. C., 2019, 192, 140-146.
[46]. 46.Adonin, S. A.; Frolova, L. A.; Sokolov, M. N.; Shilov, G. V.; Korchagin.; et al. Antimony (V) Complex Halides: Lead-Perovskite-Like Materials for Hybrid Solar Cells. Adv. Energy Mater. 2018, 8, 1701140.
[47]. 47.Li, Y.; Xu, Z.; Liu, X.; Tao.; et al. Two Heteromorphic Crystals of Antimony-Based Hybrids Showing Tunable Optical Band Gaps and Distinct Photoelectric Responses. Inorg. Chem. 2019, 58, 6544−6549
[48]. 48.Jia, X.; Ding, L. A Low-temperature Solution-processed Copper Antimony Iodide Rudorffite for Solar Cells. Sci. China Mater. 2019, 62, 54−58.
[49]. 49.Vargas, B.; Ramos, E.; Perez- Gutierrez, E.; Alonso, J. C.; Solis-Ibarra, D. A Direct Bandgap Copper−Antimony Halide Perovskite. J. Am. Chem. Soc. 2017, 139, 9116−9119.
[50]. 50.Nie, R.; Mehta, A.; Park, B.-W.; Kwon, H.-W.; Im, J.; Seok, S. I. Mixed sulfur and iodide-based lead-free perovskite solar cells. J. Am. Chem. Soc. 2018, 140, 872−875.
[51]. 51.Bonabi Naghadeh S, Luo B, Abdelmageed G, Pu Y-C, Zhang C and Zhang JZ, Photophysical properties and improved stability of organic–inorganic perovskite by surface passivation. J Phys Chem C 122:15799–15818 (2018).
[52]. 52.Kopacic I, Friesenbichler B, Hoefler SF, Kunert B, Plank H, Rath T et al., Enhanced performance of germanium halide perovskite solar cells through compositional engineering. ACS Appl Energy Mater 1: 343–347 (2018).
[53]. 53.Xu H, Jiang Y, He T, Li S, Wang H, Chen Y et al., Orientation regulation of tin-based reduced-dimensional perovskites for highly efficient and stable Photovoltaics. Adv Funct Mater 29:1807696 (2019).
[54]. 54.Yu B-B, Liao M, Yang J, Chen W, Zhu Y, Zhang X et al., Alloy-induced phase transition and enhanced

photovoltaic performance: the case of Cs3Bi2I9−xBrx perovskite solar cells. J Mater Chem A 7:8818–8825 (2019).

[55]. 55.Xu X, Chueh C-C, Yang Z, Rajagopal A, Xu J, Jo SB et al., Ascorbic acid as an effective antioxidant additive to enhance the efficiency and stability of Pb/Sn-based binary perovskite solar cells. Nano Energy 34:392–398 (2017).

[56]. 56.Tai Q, Guo X, Tang G, You P, Ng T-W, Shen D et al., Antioxidant grain passivation for air-stable tin-based perovskite solar cells. Angew Chem Int Ed 58:806–810 (2019).

[57]. 57.Dubey A, Adhikari N, Mabrouk S, Wu F, Chen K, Yang S et al., A strategic review on processing routes towards highly efficient perovskite solar cells. J Mater Chem A 6:2406–2431 (2018).

[58]. 58.Zhang, S.; Ye, L.; Zhao, W.; Yang, B.; Wang, Q.; Hou, J. Realizing over 10% efficiency in polymer solar cell by device optimization. Sci. China Chem. 2015, 58, 248–256.

[59]. 59.Gao, K.; Zhu, Z.; Xu, B.; Jo, S.; Kan, Y.; Peng, X.; Jen, A.K. Highly Efficient Porphyrin-Based OPV/Perovskite Hybrid Solar Cells with Extended Photoresponse and High Fill Factor. Adv. Mater. 2017, 29, 1703980.